

# Simulating the Smallest Ring World of Chariklo

Shugo Michikoshi, and Eiichiro Kokubo

michikos@ccs.tsukuba.ac.jp, and kokubo@th.nao.ac.jp

## ABSTRACT

A ring system consisting of two dense narrow rings has been discovered around Centaur Chariklo. The existence of these rings around a small object poses various questions, such as their origin, stability, and lifetime. In order to understand the nature of Chariklo's rings, we perform global  $N$ -body simulations of the self-gravitating collisional particle rings for the first time. We find that Chariklo should be denser than the ring material to avoid the rapid diffusion of the rings. If Chariklo is denser than the ring material, fine spiral structures called self-gravity wakes occur in the inner ring. These wakes accelerate the viscous spreading of the ring significantly and they typically occur on timescales of about 100 years for m-sized ring particles, which is considerably shorter than the timescales suggested in previous studies. The existence of these narrow rings implies smaller ring particles or the existence of shepherding satellites.

## 1. Introduction

Recently, two dense narrow rings around Centaur Chariklo were discovered by occultation observation (Braga-Ribas et al. 2014). A ring around Centaur Chiron was also proposed (Ruprecht et al. 2015; Ortiz et al. 2015). These observations suggest that rings around large Centaurs may not be as rare as previously thought.

Several mechanisms for the formation of Chariklo's rings have been proposed: collisional ejection from the parent body, satellite disruption, and out gassing (Pan & Wu 2016). The tidal disruption of a differentiated object during a close encounter with a giant planet can also result in the formation of a ring (Hyodo et al. 2016). From the numerical integration of the Chariklo orbit it was suggested that the possibility of a close encounter with a giant planet that is able to disrupt Chariklo's rings is low (Araujo et al. 2016). The formation mechanism of the rings is still not well understood. In order to understand the origin of the ring system, we need to investigate the ring structure in detail.

---

<sup>1</sup> Center for Computational Sciences, University of Tsukuba, Tsukuba, Ibaraki 305-8577, Japan

<sup>2</sup> Division of Theoretical Astronomy, National Astronomical Observatory of Japan, Osawa, Mitaka, Tokyo 181-8588, Japan

Observations have found a difference in the inner ring widths between ingress and egress (Braga-Ribas et al. 2014). The width variation indicates that the inner ring has a finite eccentricity. On the other hand, Chariklo has large oblateness, which should lead to the rapid differential precession of the ring, resulting in a circular ring. Thus, there must be some mechanism keeping the ring eccentricity. To explain the eccentric ring around Uranus, apse alignment due to ring self-gravity has been proposed (Goldreich & Tremaine 1979a,b). By applying the same model to Chariklo’s rings, the ring mass and particle size have been estimated (Pan & Wu 2016). From these estimates, they found that the inner ring is slightly gravitationally unstable in the context of Toomre stability (Toomre 1964).

Local  $N$ -body simulations of Saturn’s rings revealed that self-gravity wakes exist in Saturn’s A and B rings (e.g., Salo 1992, 1995; Michikoshi & Kokubo 2011; Michikoshi et al. 2015). The self-gravity wakes are non-axisymmetric small spiral structures formed by gravitational instability, which enable efficient angular momentum transfer. Thus, it is important to elucidate whether self-gravity wakes exist in Chariklo’s rings. The optical depth in Chariklo’s inner ring is about 0.38, which is marginal for the formation of self-gravity wakes (Salo 1995). The critical optical depth for the formation of self-gravity wakes depends on the distance from the central body and the properties of the ring particles. In order to investigate Chariklo’s ring system, we perform global  $N$ -body simulations of the two narrow rings with full self-gravity for the first time. Section 2 describes the model and the simulation method, Section 3 presents the results of the numerical simulations, and Section 4 contains a summary and a discussion.

## 2. Simulation Method

Chariklo has a large oblateness of about 0.2 (Braga-Ribas et al. 2014), resulting in a large gravitational moment  $J_2$ , which causes the differential precession of the rings. We here focus on the formation of structures over the dynamical timescale. Thus, we neglect the oblateness. The latest observations and analysis show that Chariklo has a shape with volume equivalent to a sphere of radius 125 km and its density is 0.8 or 1.2 g cm<sup>-3</sup> (Leiva et al. 2016). We adopt a spherical Chariklo with radius 125 km and density  $\rho_C = 1.0$  g cm<sup>-3</sup>. Chariklo has the inner dense ring, with different optical depths and radial widths for the ingress ( $W = 6.16$  km,  $\tau = 0.449$ ) and egress ( $W = 7.17$  km,  $\tau = 0.317$ ). This indicates that the inner ring may have a finite eccentricity. However, in this paper, we assume that the inner ring is circular and uniform with  $W = 6.7$  km and  $\tau = 0.38$  as a first step. Similarly, we assume that the outer ring is circular and uniform with  $W = 3.5$  km and  $\tau = 0.06$ . The inner and outer rings are located at distances of  $a = 390.6$  km and 404.8 km from the center of Chariklo, respectively.

The properties of ring particles are not well constrained. For the sake of simplicity, we assume that all particles have the same mass  $m_p$  and radius  $r_p$ . In Saturn’s rings, the typical particle size varies between a centimeter and a few meters (French & Nicholson 2000). Furthermore, considering the apse alignment of the ring by its self-gravity, Pan & Wu (2016) estimated the ring mass,

which corresponds to a few meter-sized particles. We assume  $r_p = 2.5\text{--}10\text{ m}$ , and density ratios  $\rho_p/\rho_C = 0.05, 0.10, 0.25, 0.50, 0.75$ , and  $1.00$ . The number of ring particles is 21 to 345 million. The basic ring dynamics is controlled by the two non-dimensional ring parameters  $\tau$  and  $\tilde{r}_H$ , where  $\tilde{r}_H$  is the scaled Hill radius of ring particles given by  $\tilde{r}_H = r_H/2r_p$  with  $r_H = (2m_p/3M_C)^{1/3}a$  (Salo 1995), where  $M_C$  is Chariklo’s mass. Note that  $\tilde{r}_H$  is independent of the particle size.

The equation of motion of particle  $i$  is

$$\frac{d^2\mathbf{r}_i}{dt^2} = -GM_C \frac{\mathbf{r}_i}{|\mathbf{r}_i|^3} - \sum_{j \neq i} Gm_p \frac{\mathbf{r}_{ij}}{(r_{ij}^2 + \epsilon_g^2)^{3/2}} + \mathbf{f}_{\text{col}}, \quad (1)$$

where  $\mathbf{r}_i$  is the position vector of particle  $i$ ,  $\mathbf{r}_{ij} = \mathbf{r}_i - \mathbf{r}_j$ ,  $r_{ij} = |\mathbf{r}_{ij}|$ ,  $\epsilon_g$  is the softening length, and  $\mathbf{f}_{\text{col}}$  is the collisional force. We adopt the soft sphere model as the collision model (Salo 1995). In this model, a collision is described as a damped oscillation. This model has a free parameter, the collision duration  $t_{\text{col}}$ , which should be sufficiently shorter than the dynamical timescale. The collision duration is  $t_{\text{col}} = 0.0025t_K$ , where  $t_K$  is the orbital period. The restitution coefficient is  $\epsilon = 0.1$ . We set  $\epsilon_g = 0.1r_p$ .

We integrate the equation of motion with the leapfrog method. To reduce the computational time, as in Salo (1995), we consider two different timesteps,  $\Delta t_{\text{grav}}$  and  $\Delta t_{\text{col}}$ . The timestep  $\Delta t_{\text{col}}$  is for collisions, and we integrate the equation of motion with  $\Delta t_{\text{col}}$ . We update the gravitational acceleration with  $\Delta t_{\text{grav}}$ , which is set to be longer than  $\Delta t_{\text{col}}$ . We adopt  $\Delta t_{\text{grav}} = 0.005t_K$ , which is sufficiently small for resolving gravitational interactions among particles, and  $\Delta t_{\text{col}} = \Delta t_{\text{grav}}/32 = t_{\text{col}}/16$ . We use the tree algorithm for the gravitational force calculation (Barnes & Hut 1986). We adopt the opening angle  $\theta = 0.5$ , and employ the  $N$ -body simulation library, Framework for Developing Particle Simulator (FDPS) (Iwasawa et al. 2016) with the Phantom-GRAPe module (Tanikawa et al. 2012, 2013).

### 3. Results

#### 3.1. Formation of Self-gravity Wakes

Figure 1 shows the ring at  $t = 10t_K$ , where  $\rho_p/\rho_C = 0.50$  and  $r_p = 5\text{ m}$ ; no large-scale structures are visible. For dynamical timescales, the ring keeps its original global shape. However, we find small-scale structures, namely, self-gravity wakes, in the inner ring (Fig. 2). Initially, the ring particles are distributed uniformly. At  $t = 1t_K$ , fluctuations in the ring surface density grow due to gravitational instability, and self-gravity wakes form at  $t = 2t_K$ . After  $t = 3t_K$ , the self-gravity wakes are formed and destroyed continuously. The self-gravity and collision of particles form particle aggregates, while the differential rotation tears them apart. These competing processes are the cause of self-gravity wakes.

The spatial scale of self-gravity wakes is characterized by the critical wavelength of the gravi-

tational instability (Toomre 1964; Salo 1995; Daisaka & Ida 1999)

$$\lambda_{\text{cr}} = \frac{4\pi^2 G \Sigma}{\Omega^2} = 0.36 \left( \frac{a_i}{390.6 \text{ km}} \right)^3 \left( \frac{r_C}{125 \text{ km}} \right)^{-3} \left( \frac{\rho_p/\rho_C}{0.5} \right) \left( \frac{\tau}{0.38} \right) \left( \frac{r_p}{5 \text{ m}} \right) \text{ km}, \quad (2)$$

where  $\Sigma$  is the ring surface density and  $\Omega = 2\pi/t_K$  is the Kepler angular frequency.

On the other hand, in the outer ring, the self-gravity wakes do not develop. Since the optical depth in the outer ring is small, the energy dissipation by collisions is insufficient. Thus, the random velocity of ring particles is high and the ring is gravitationally stable. Since the outer ring is near the Roche limit, small aggregates are visible. The tidal force is comparable with their self-gravity. Thus they may be temporal.

### 3.2. Ring Particle Properties

We constrain the properties of ring particles with those of the self-gravity wakes. Figure 3 shows the structure of the rings at  $t = 10 t_K$  for the models where  $\rho_p/\rho_C = 0.05, 0.10, 0.25, 0.50, 0.75$  and  $1.00$  with  $r_p = 5 \text{ m}$ . In the  $\rho_p/\rho_C = 0.75$ , and  $1.00$  models, large particle aggregates form and the ring spreads rapidly over the dynamical timescale. Thus, this model may not correspond to the real ring. The scaled Hill radius determines whether a particle pair can gravitationally bind (Ohtsuki 1993; Salo 1995; Karjalainen & Salo 2004), which is given as

$$\tilde{r}_H = 1.36 \left( \frac{a}{390.6 \text{ km}} \right) \left( \frac{r_C}{125 \text{ km}} \right)^{-1} \left( \frac{\rho_p}{\rho_C} \right)^{1/3}. \quad (3)$$

Studies of Saturn’s rings showed that gravitationally bound aggregates form if  $\tilde{r}_H \gtrsim 1.1$  (Ohtsuki 1993; Salo 1995; Karjalainen & Salo 2004). Therefore, the necessary condition for ring formation is  $\rho_p/\rho_C < 0.52$ , in other words, the particle density should be lower than half of that of Chariklo.

In the inner ring, self-gravity wakes appear for  $\rho_p/\rho_C = 0.25$  and  $0.5$ , while they do not appear for  $\rho_p/\rho_C = 0.05$  and  $0.1$ . As the particle density increases, the spatial scale of the self-gravity wakes increases, as shown in Equation (2). For  $\tau = 0.38$ , the self-gravity wakes form under the condition  $0.65 \lesssim \tilde{r}_H \lesssim 1.1$  (Salo 1995; Ohtsuki & Emori 2000; Daisaka et al. 2001), which is independent of the particle radius. If  $\tilde{r}_H \lesssim 0.65$ , the self-gravity wake formation is suppressed, which corresponds to  $\rho_p/\rho_C < 0.11$ . If Chariklo has the typical Centaur density,  $\rho_C \simeq 1.0 \text{ g cm}^{-3}$ , the particle density needs to be less than  $0.1 \text{ g cm}^{-3}$  for the suppression of self-gravity wakes.

Figure 4 shows the dependence of the spatial scale of self-gravity wakes on  $r_p$  with  $\rho_p/\rho_C = 0.5$ ,  $r_p = 2.5, 5, 7.5$ , and  $10 \text{ m}$ . In all the models, the self-gravity wakes develop, which is consistent with the condition for self-gravity wake formation discussed above. As indicated by Equation (2), the spatial scale increases with  $r_p$ . The ring width for larger particles is wider than that with smaller particles. This is because the viscosity due to self-gravity wakes increases with wake size.

The Chariklo ring was discovered by stellar occultation (Braga-Ribas et al. 2014). The projected star radius for Chariklo was estimated at around  $1 \text{ km}$ . Figure 5 shows a simulation of the

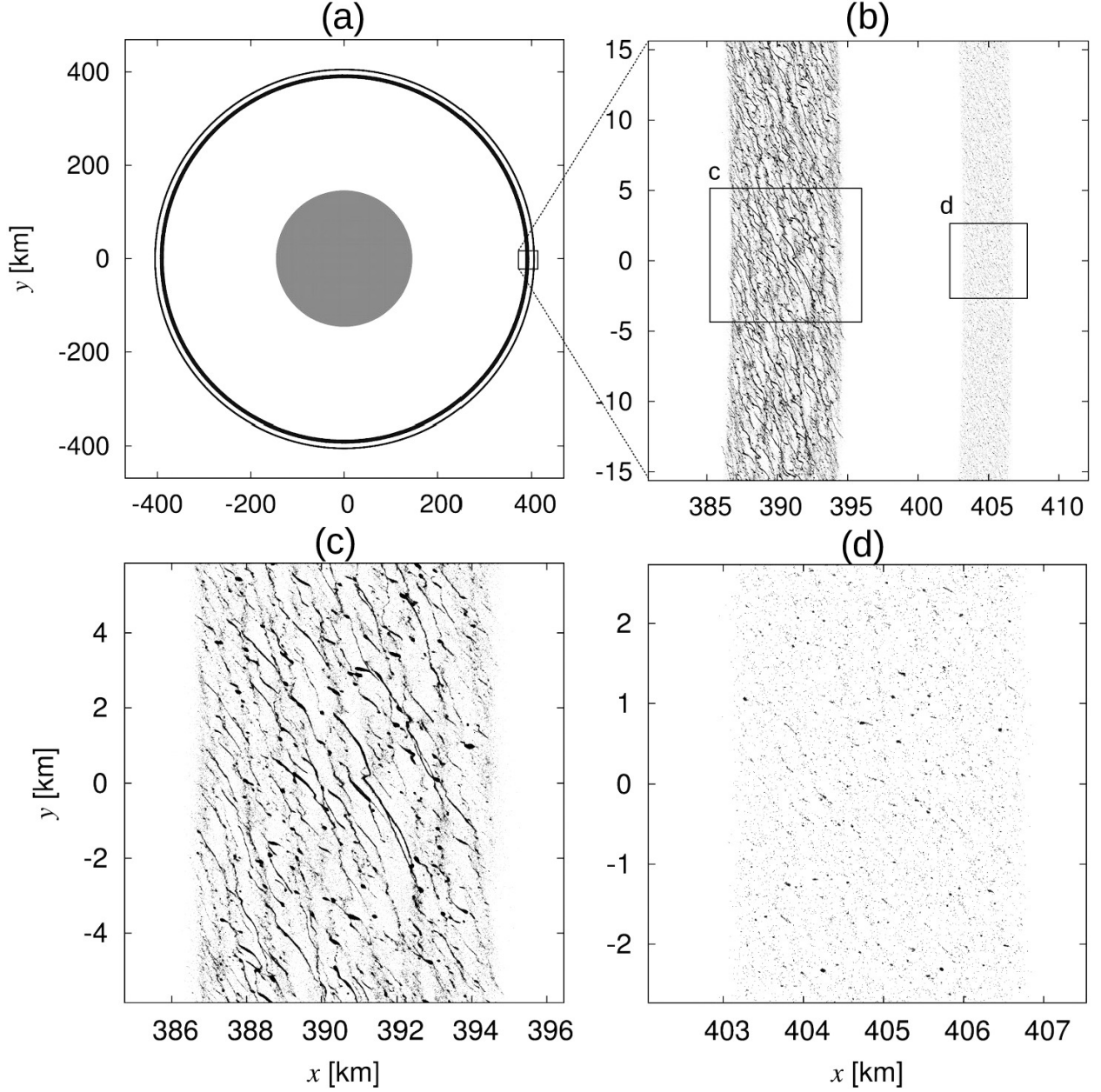


Fig. 1.— Snapshots of the simulated ring in the  $x$ - $y$  plane at  $t = 10t_K$ , where the particle density and radius are  $\rho_p/\rho_C = 0.5$  and  $r_p = 5$  m, respectively. The left panel (a) shows the overall structure of the ring, while the panels (b), (c), (d) show enlarged views of ring sections.

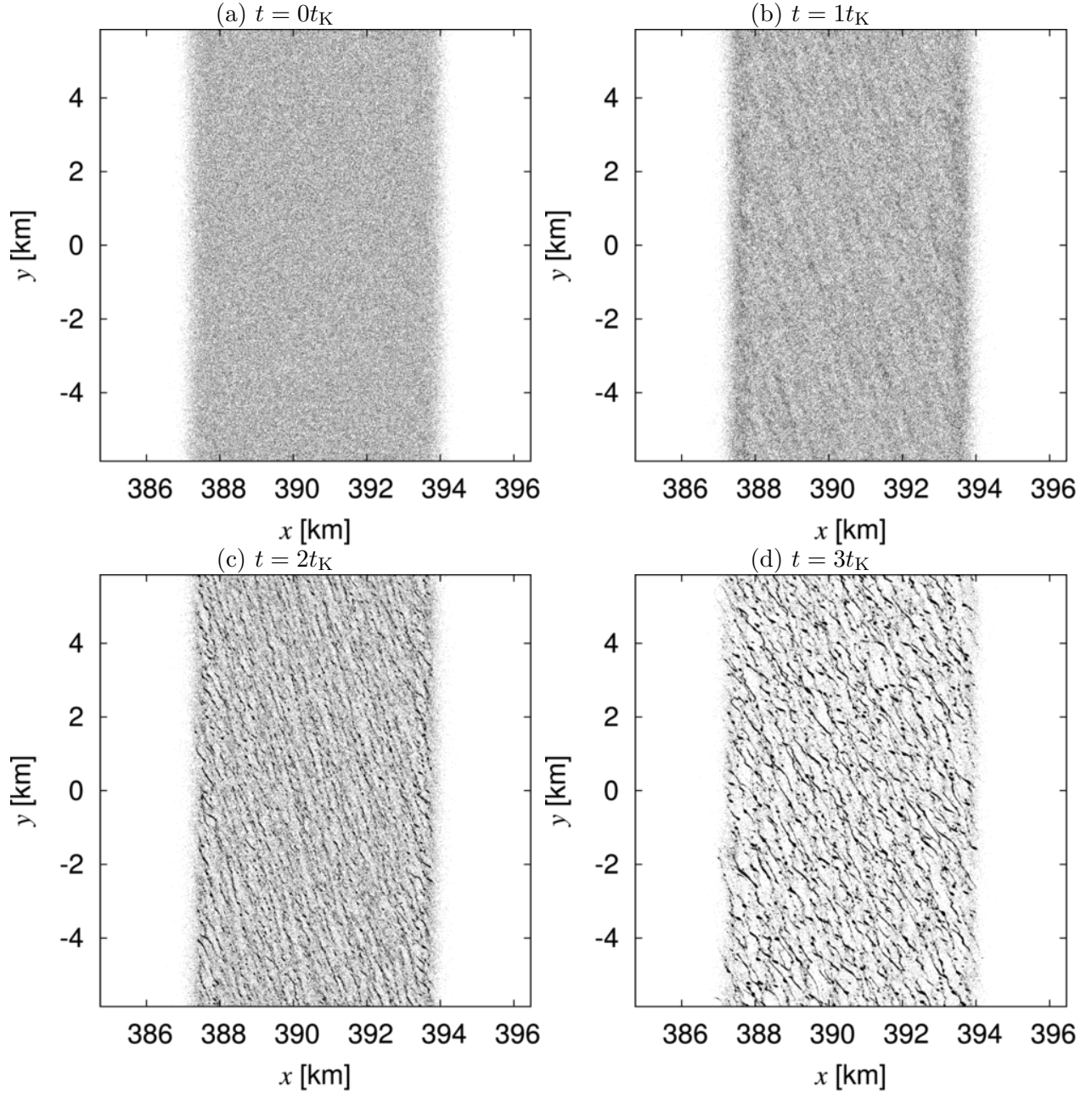


Fig. 2.— Snapshots of the inner ring at (a)  $t = 0$ , (b)  $1t_K$ , (c)  $2t_K$ , and (d)  $3t_K$  for the model with  $\rho_p/\rho_C = 0.5$  and  $r_p = 5$  m.

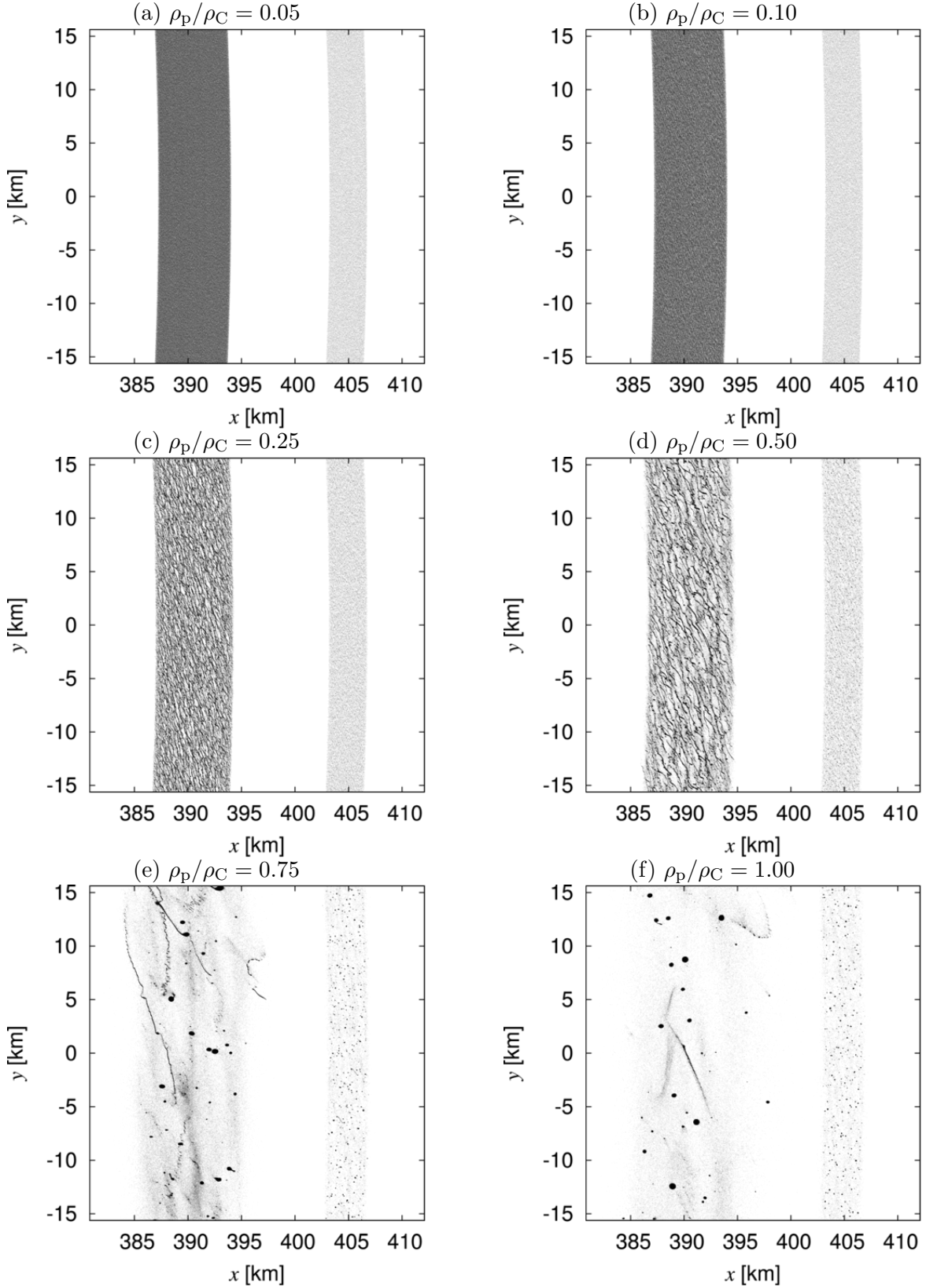


Fig. 3.— Snapshots of the inner ring at  $t = 10t_K$  for the models with (a)  $\rho_p/\rho_C = 0.05$ , (b) 0.1, (c) 0.25, (d) 0.50, (e) 0.75, and (f) 1.0 with  $r_p = 5$  m.

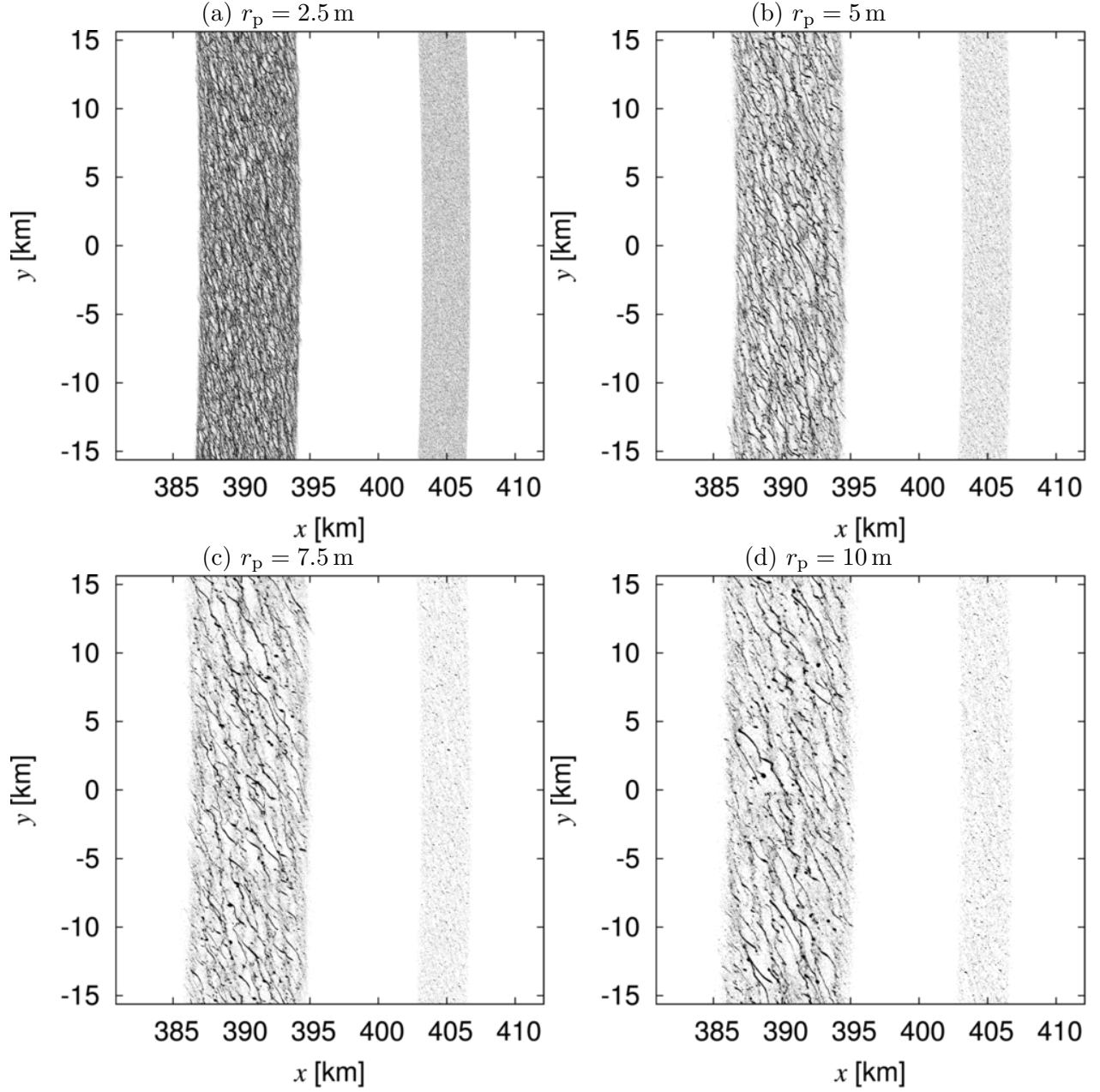


Fig. 4.— Snapshots of the inner ring at  $t = 10t_K$  for the models with (a)  $r_p = 2.5$  m, (b) 5 m, (c) 7.5 m, and (d) 10 m with  $\rho_p/\rho_C = 0.50$ .



dynamical optical depth  $\tau = 4\Sigma/3r_p\rho_p$  with spatial resolutions with radii  $\Delta r = 0.25, 0.50$ , and  $1.0$  km for the model where  $\rho_p/\rho_C = 0.5$  and  $r_p = 10$  m. The critical wavelength is  $\lambda_{cr} = 0.72$  km. We can observe fluctuations due to self-gravity wakes in the  $\Delta r = 0.25$  km and  $0.5$  km models, while the optical depth is almost smooth in the  $\Delta r = 1.0$  km model. If the spatial scale of self-gravity wakes is larger than the star projected radius, the fluctuation due to self-gravity wakes may be detected by occultation observations. However, the observations show the smooth distribution. Thus, the spatial scale of self-gravity wakes would be smaller than  $1$  km, which leads to

$$r_p \lesssim 13.7 \left( \frac{\rho_p/\rho_C}{0.5} \right)^{-1} \left( \frac{\tau}{0.38} \right)^{-1} \text{ m}, \quad (4)$$

which is consistent with the estimate by Pan & Wu (2016). In future observations, if we detect spatial variation of the optical depth, this will confirm the existence of self-gravity wakes and give a lower boundary for the particle size.

If we consider the ring mass estimated by Pan & Wu (2016), we can give the lower boundary of the particle size. The surface density is estimated as  $\text{few} \times 100 \text{ g cm}^{-2}$  from the apse alignment argument. From the ring formation criterion  $\rho_p/\rho_C < 0.52$ , we give the following constraint

$$r_p \gtrsim 3.8 \left( \frac{\Sigma}{100 \text{ g cm}^{-2}} \right) \text{ m}. \quad (5)$$

### 3.3. Ring Lifetime

The self-gravity wakes cause efficient radial diffusion in the inner ring. The effective viscosity of self-gravity wakes was obtained by  $N$ -body simulations (Daisaka et al. 2001; Tanaka et al. 2003), which is given as  $\nu_{sgw} \simeq 26\tilde{r}_H^5 G^2 \Sigma^2 / \Omega^3$ . Using this, we obtain the diffusion time of the inner ring as

$$t_{\text{inner}} \equiv \frac{W^2}{\nu} \simeq 113 \left( \frac{r_p}{1 \text{ m}} \right)^{-2} \left( \frac{\rho_p}{0.5 \text{ g cm}^{-3}} \right)^{-11/3} \text{ years}, \quad (6)$$

where we assume  $W = 6.7$  km,  $\tau = 0.38$ , and  $a = 390.6$  km. This diffusion time is much shorter than in previous studies (Braga-Ribas et al. 2014; Pan & Wu 2016) where the self-gravity wakes are not taken into account.

For the outer ring we estimate the diffusion time using the collisional viscosity,  $\nu_{col} \simeq r_p^2 \Omega \tau$ , which is

$$t_{\text{outer}} \simeq 7.1 \times 10^4 \left( \frac{r_p}{1 \text{ m}} \right)^{-2} \text{ years}, \quad (7)$$

where we assume  $W = 3.5$  km,  $\tau = 0.06$ , and  $a = 404.8$  km. This is roughly consistent with the results of previous studies (Braga-Ribas et al. 2014; Pan & Wu 2016).

Equation (6) shows that the lifetime of the inner ring is much shorter than the typical dynamical lifetime of Centaurs,  $\sim 10^6$  years, if the particle size is on the order of  $1$  m. If the rings were formed

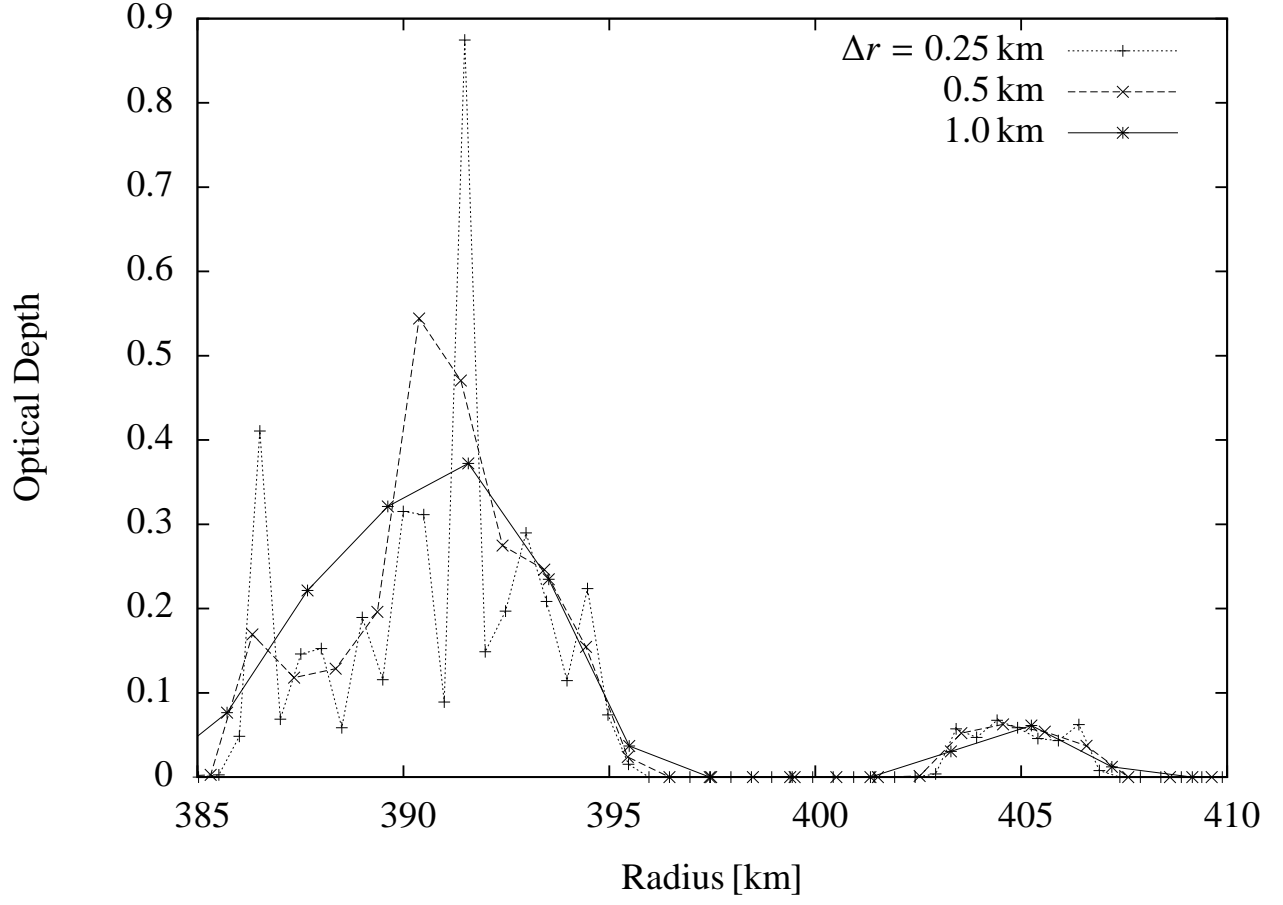


Fig. 5.— Simulation of the dynamical optical depth along the line  $y = 0$  at  $t = 10 t_K$  for the model where  $\rho_p/\rho_C = 0.5$  and  $r_p = 10$  m. The spatial resolutions are  $\Delta r = 0.25$  km (dotted),  $\Delta r = 0.5$  km (dashed), and 1.0 km (solid).

at the same time when Chariklo was scattered into the Centaur region, this significantly short ring lifetime would be inconsistent. One possible solution to this contradiction is that Chariklo’s rings are very young. Another solution is that the ring consists of small particles, such as particles of less than 1 cm. It is also possible that the narrow ring is due to shepherding satellites, which will be discussed below (Braga-Ribas et al. 2014).

#### 4. Summary and Discussion

We performed global  $N$ -body simulations of Chariklo’s rings and investigated their structure. We found that in order for Chariklo to host rings instead of particle aggregates its density should be larger than that of particles. Under this condition, the self-gravity wakes inevitably develop in the inner ring independently of the particle size, while their spatial scale depends on the particle size. For m-sized ring particles, the timescale of ring viscous spreading due to the self-gravity wakes is on the order of 100 years, which is much shorter than that estimated in previous studies (Braga-Ribas et al. 2014; Pan & Wu 2016).

Our simulations predict that Chariklo is denser than the ring particles, and the ring particles are also less dense than ice, similar to Saturn’s rings. In Saturn’s rings, from comparisons of observations and  $N$ -body simulations, a particle density less than that of ice has been proposed (Salo et al. 2004; Michikoshi et al. 2015). The higher density of Chariklo than that of the ring particles suggests that Chariklo may have a dense core. Previous studies have hypothesized that the ring material originates from the stripped icy mantle of a differentiated body (Hyodo et al. 2016), which is consistent with our findings.

The timescale of viscous ring spreading (Equation (6)) suggests three possibilities: a very young ring ( $\sim 1$ –100 years), smaller ring particles, or existence of shepherding satellites. If the ring is young, because a close encounter with a giant planet is rare (Araujo et al. 2016), the ring formation by the tidal interaction with giant planets may be difficult. Then the other mechanisms, such as out gassing, would be preferable (Pan & Wu 2016). If the ring particles are smaller than  $\sim 1$  cm, the inner ring can last longer than  $10^6$  years. However, this small particle size is inconsistent with the estimate from the apse alignment of the ring (Pan & Wu 2016). For the m-sized particles the existence of shepherding satellites is required to counteract the viscous ring spreading. The minimum mass of the shepherding satellite depends on the distance from the inner ring edge  $d$  and the particle size and density (Goldreich & Tremaine 1982),

$$M_s \simeq 4.1 \left( \frac{\nu d^3}{\Omega a^5} \right)^{1/2} M_C = 1.3 \times 10^{17} \left( \frac{d}{100 \text{ km}} \right)^{3/2} \left( \frac{\rho_p}{0.5 \text{ g cm}^{-3}} \right)^{11/6} \left( \frac{r_p}{1 \text{ m}} \right) \text{ g}, \quad (8)$$

where we assumed the viscosity due to the self-gravity wakes, which is  $\nu \propto \Sigma^2$ . The size of a satellite with mass  $10^{17}$  g is on the order of kilometers. Furthermore, the shepherding satellite hypothesis may be preferable because it could also explain the ring eccentricity.

The particle size is a key parameter for determining the dynamical property of Chariklo’s rings. However, the particle size has not yet been constrained observationally. In future, if the self-gravity wakes are detected by higher resolution occultation observations, they will be able to provide a lower limit for the particle size.

Our simulations suggest that the formation of self-gravity wakes is a general process in dense narrow rings. For example, the Huygens ringlet in the Cassini division of Saturn’s ring and the  $\epsilon$  ring of Uranus have a sufficiently high optical depth to form self-gravity wakes. However, their spatial scale is far below the observational limit today.

In this study, we assumed the circular ring, though the inner ring may have a finite eccentricity. The effect of the eccentricity on the self-gravity wake dynamics has not been examined. In the subsequent work, we plan to investigate its effect with more realistic ring models considering, for example, the size distribution of particles, the restitution coefficient that depends on the collisional velocity (Bridges et al. 1984), and shepherding satellites.

Numerical computations were carried out on ATERUI (Cray XC30) at the Center for Computational Astrophysics, National Astronomical Observatory of Japan.

## REFERENCES

- Araujo, R. A. N., Sfair, R., & Winter, O. C. 2016, *ApJ*, 824, 80
- Barnes, J. & Hut, P. 1986, *Nature*, 324, 446
- Braga-Ribas, F., Sicardy, B., Ortiz, J. L., Snodgrass, C., Roques, F., Vieira-Martins, R., Camargo, J. I. B., Assafin, M., Duffard, R., Jehin, E., Pollock, J., Leiva, R., Emilio, M., Machado, D. I., Colazo, C., Lellouch, E., Skottfelt, J., Gillon, M., Ligier, N., Maquet, L., Benedetti-Rossi, G., Gomes, A. R., Kervella, P., Monteiro, H., Sfair, R., El Moutamid, M., Tancredi, G., Spagnotto, J., Maury, A., Morales, N., Gil-Hutton, R., Roland, S., Ceretta, A., Gu, S.-H., Wang, X.-B., Harpsøe, K., Rabus, M., Manfroid, J., Opitom, C., Vanzi, L., Mehret, L., Lorenzini, L., Schneider, E. M., Melia, R., Lecacheux, J., Colas, F., Vachier, F., Widemann, T., Almenares, L., Sandness, R. G., Char, F., Perez, V., Lemos, P., Martinez, N., Jørgensen, U. G., Dominik, M., Roig, F., Reichart, D. E., Lacluyze, A. P., Haislip, J. B., Ivarsen, K. M., Moore, J. P., Frank, N. R., & Lambas, D. G. 2014, *Nature*, 508, 72
- Bridges, F. G., Hatzes, A., & Lin, D. N. C. 1984, *Nature*, 309, 333
- Daisaka, H. & Ida, S. 1999, *Earth, Planets, and Space*, 51, 1195
- Daisaka, H., Tanaka, H., & Ida, S. 2001, *Icarus*, 154, 296
- French, R. G. & Nicholson, P. D. 2000, *Icarus*, 145, 502
- Goldreich, P. & Tremaine, S. 1979a, *AJ*, 84, 1638

- . 1979b, *Nature*, 277, 97
- . 1982, *ARA&A*, 20, 249
- Hyodo, R., Charnoz, S., Genda, H., & Ohtsuki, K. 2016, *ApJ*, 828, L8
- Iwasawa, M., Tanikawa, A., Hosono, N., Nitadori, K., Muranushi, T., & Makino, J. 2016, *PASJ*, 68, 54
- Karjalainen, R. & Salo, H. 2004, *Icarus*, 172, 328
- Leiva, R., Sicardy, B., Berard, D., Meza Quispe, E., camargo, j., Assafin, M., Braga-Ribas, F., Vieira-Martins, R., Maquet, L., Colas, F., Sickafoose, A. A., Bath, K.-L., & Dauvergne, J.-L. 2016, in *AAS/Division for Planetary Sciences Meeting Abstracts*, Vol. 48, *AAS/Division for Planetary Sciences Meeting Abstracts*, 203.07
- Michikoshi, S., Fujii, A., Kokubo, E., & Salo, H. 2015, *ApJ*, 812, 151
- Michikoshi, S. & Kokubo, E. 2011, *ApJ*, 732, L23+
- Ohtsuki, K. 1993, *Icarus*, 106, 228
- Ohtsuki, K. & Emori, H. 2000, *AJ*, 119, 403
- Ortiz, J. L., Duffard, R., Pinilla-Alonso, N., Alvarez-Candal, A., Santos-Sanz, P., Morales, N., Fernández-Valenzuela, E., Licandro, J., Campo Bagatin, A., & Thirouin, A. 2015, *A&A*, 576, A18
- Pan, M. & Wu, Y. 2016, *ApJ*, 821, 18
- Ruprecht, J. D., Bosh, A. S., Person, M. J., Bianco, F. B., Fulton, B. J., Gulbis, A. A. S., Bus, S. J., & Zangari, A. M. 2015, *Icarus*, 252, 271
- Salo, H. 1992, *Nature*, 359, 619
- . 1995, *Icarus*, 117, 287
- Salo, H., Karjalainen, R., & French, R. G. 2004, *Icarus*, 170, 70
- Tanaka, H., Ohtsuki, K., & Daisaka, H. 2003, *Icarus*, 161, 144
- Tanikawa, A., Yoshikawa, K., Nitadori, K., & Okamoto, T. 2013, *New A*, 19, 74
- Tanikawa, A., Yoshikawa, K., Okamoto, T., & Nitadori, K. 2012, *New A*, 17, 82
- Toomre, A. 1964, *ApJ*, 139, 1217